

# Subsoil classification and geotechnical zonation for Guadalajara City, México: $V_{s30}$ , soil fundamental periods, 3D structure and profiles

Alejandro Ramírez Gaytan<sup>1</sup>, Hortencia Flores Estrella<sup>2\*</sup>, Adolfo Preciado<sup>3</sup>, William L. Bandy<sup>4</sup>, Salvador Lazcano<sup>5</sup>, Leonardo Alcántara Nolasco<sup>6</sup>, Jorge Aguirre González<sup>6</sup> and Michael Korn<sup>7</sup>

<sup>1</sup>Departamento de Ciencias Computacionales CUCEI, UdeG, Marcelino García Barragán 1421, 44430 Guadalajara, Mexico, <sup>2</sup>Department of Applied Geophysics, Institute of Applied Geosciences, TU Berlin, Ernst-Reuter-Platz 1, 10587 Berlin, Germany, <sup>3</sup>Departamento del Hábitat y Desarrollo Urbano, Instituto Tecnológico y de Estudios Superiores de Occidente (ITESO), Periférico Sur Manuel Gómez Morín 8585, 45604 Tlaquepaque, Mexico, <sup>4</sup>Instituto de Geofísica, Universidad Nacional Autónoma de México, Circuito Interior, Ciudad Universitaria, Coyoacán, 04510 Mexico City, Mexico, <sup>5</sup>Suelo Estructura, Construction Company, Cauda 946-1, Jardines del Bosque, 44520 Guadalajara, Mexico, <sup>6</sup>Instituto de Ingeniería, Universidad Nacional Autónoma de México, Circuito Interior, Ciudad Universitaria, Coyoacán, 04510 Mexico City, Mexico, and <sup>7</sup>Institute for Geophysics and Geology, Leipzig University, Talstr. 35, 04103 Leipzig, Germany

Received March 2019, revision accepted December 2019

## ABSTRACT

Guadalajara, Jalisco, is the second largest city in Mexico with around 4.5 million inhabitants. A high seismic hazard exists in the city due to forces produced by the interaction between the Rivera, Cocos and North American plates and the smaller Jalisco Block. Guadalajara is one of the largest cities built over pumice soil deposits. Furthermore, the near-surface phreatic level causes a high susceptibility to liquefaction. All these features can cause extreme earthquake site effects. Due to the fragile inner structure of pumice sands, traditional geotechnical tests are inappropriate to characterize the seismic response. Therefore, we propose the use of surface wave analysis methods (multichannel analysis of surface waves and refraction microtremor), which we applied in 33 sites to define the soil classification in terms of  $V_{s30}$  (the average shear wave velocity between the surface and 30 m depth), the bedrock depth and the fundamental period. From the soil classification, we construct a microzonation map consisting of four geotechnical zones, which we superimpose on the known construction systems within the city. The comparison between the construction period of the buildings and the fundamental frequencies of the soil indicates a high vulnerability to resonance in 1- to 4-storied old buildings constructed of adobe and unreinforced masonry within zones II and III, followed by a medium vulnerability to seismic resonance in compact buildings of 1–4 stories within zone I and 1–12 stories within zones II and IV.

**Key words:** Near-surface, Seismic, Geotechnical.

## 1 INTRODUCTION

Guadalajara is located in a region where three different tectonic plates interact (Fig. 1) and three active seismic regions

surround it: the Pacific subduction region, the Jalisco Block and its boundaries and the active Colima Volcanic complex. Historically, moderate and severe earthquakes have affected the city (García and Suárez 1996; Zobin and Ventura 1998; Lazcano 2001; Ramírez-Gaytan, Aguirre and Huerta 2010; Quitanar *et al.* 2010; Preciado 2011; Suter 2015, 2017;

\*E-mail: h.florestrella@tu-berlin.de

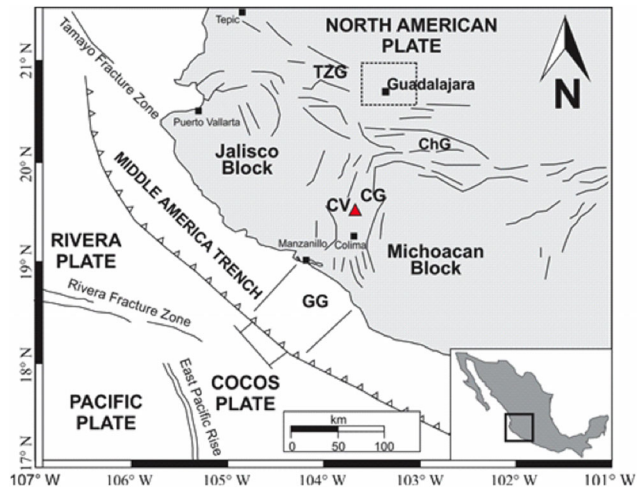


**Figure 1** Tectonic map and seismic sources around Guadalajara. CV, Colima Volcano; GG, El Gordo Graben; CG, Colima Graben; ChG, Chapala Graben; TZG, Tepic-Zacoalco Graben.

Castillo-Aja and Ramírez-Herrera 2017; Ramírez-Gaytan *et al.* 2019).

Although the seismic hazard is well documented, the seismic risk has not been evaluated for the urban area of Guadalajara (e.g. Lazcano 2001, 2004, 2007, 2010). Data from seismic instrumentation are scarce, resulting in a lack of studies that evaluate the possible site effects within the city. Furthermore, microzonation maps for the entire metropolis are not available. Thus, tall buildings have been constructed without adequate subsoil zonation. Moreover, the proximity of the Jalisco Block to Guadalajara (Fig. 1) is responsible for many uncertainties regarding seismic design, which makes low-, intermediate- and high-rise buildings extremely susceptible to significant structural damage during future events.

When evaluating the seismic risk in Guadalajara, it is also necessary to consider the characteristics of the subsoil underlying Guadalajara, similar to what has been done in Mexico City which is similarly built upon loose, unconsolidated material (a lacustrine area with soft clay deposits). There, the characteristics of the subsoil have a decisive influence on the site effects produced by distant earthquakes (Flores Estrella and Aguirre Gonzalez 2003; Flores-Estrella, Lomnitz and Yussim 2007). Also, since the phreatic level is close to the surface beneath all of Guadalajara, these areas could be highly susceptible to sand liquefaction.

To better understand the seismic response in Guadalajara, in this work we propose a new geotechnical microzonation for part of the metropolitan zone. To achieve this goal, we record seismic noise at 33 sites (Fig. 2) and use surface wave

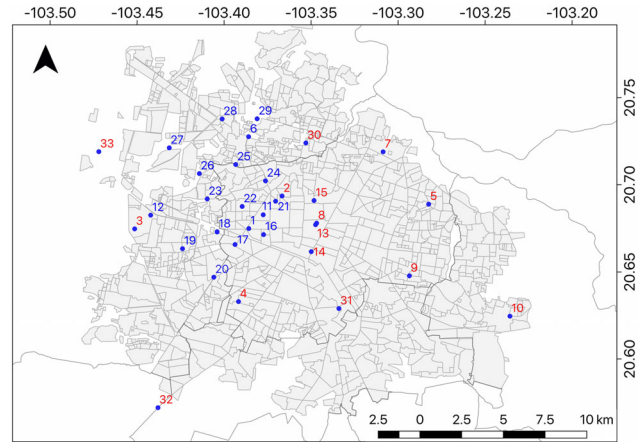


**Figure 2** Location of the 33 sites under study in Guadalajara. Sites in blue colour correspond to areas where tallest buildings are currently built. Background map is the urban area of Guadalajara (neighbourhoods, blocks and streets).

analysis methods (refraction microtremors and multichannel analysis of surface waves) to obtain near-surface velocity profiles (shear wave velocity vs. depth). From these profiles, we determine  $V_{s30}$  (the average seismic shear wave velocity between the surface and 30 m depth) and the bedrock depth, and we estimate the natural period of vibration corresponding to the fundamental soil period,  $T_s$ . Moreover, since the site response is intrinsically linked to the structural design, we superimpose the proposed geotechnical zonation with the predominant construction systems. From this analysis, we define which areas are highly susceptible to damage during a future earthquake.

This work is organized as follows. In Section 2, we describe the subsoil of Guadalajara and explain the reason why its characterization is not possible with traditional geotechnical tests. Section 3 explains the use of seismic noise to estimate velocity profiles:  $V_{s30}$ ,  $T_s$  and the bedrock depth. Sections 4 and 5 list the most important findings and discuss their implications. Finally, in Section 6, we present the conclusions and some recommendations for future research.

## 2 GUADALAJARA SUBSOIL

The subsoil in most of the Guadalajara metropolitan area has a thickness of around 100 m, distributed as follows: the uppermost 15 m is composed of a dense pumice mixture of salty sand and sandy gravel, which is followed by ~80 m of stiff, silty and pumice sand with some pumice gravel (Lazcano 2010). The underlying strata consist of limestone and sandstone, and the basement rock consists mainly of basalt

and ignimbrite. In several sites, it is possible to find 3 m of residual soils composed of red clay with gravel.

In geotechnics and soil mechanics, there are two useful parameters for characterizing soils: the internal friction angle and the compressibility. The internal friction angle is useful to estimate the soil strength and the behaviour when the soil is wet; it is a fundamental parameter in the estimation of slope stability, foundations and excavations. The compressibility is used to estimate the amount of settlement under loads. Geotechnical tests use the standard penetration test (SPT) and cone penetration test (CPT) to estimate the above parameters in order to characterize soils.

However, in the case of pumice sands the characterization by traditional geotechnical tests is extremely difficult and the results can be tenuous at best (Brooms and Floding 1988; Lazcano 1995; Lazcano 2007). This is because: (i) it is impossible to get undisturbed samples for laboratory testing due to the fragile structure of pumice soils; (ii) SPT and CPT would crush the pumice in such a way that it would not be representative of real conditions; and (iii) the compressibility of pumice soils is much higher than that of quartz sands (e.g. Wesley *et al.* 1999; Pender 2006; Pender *et al.* 2006; Mesri and Vardhanabhuti 2009).

Considering the particularities of pumice soils and the questionable use of traditional geotechnical tests for their characterization, we apply other practical and reliable methods that use passive seismic data to characterize the subsoil. These methods are multichannel analysis of surface waves (Park, Miller and Xia 1999) and refraction microtremors (Louie 2001); both are non-invasive techniques that keep the fragile structure of pumice sands unaltered and undisturbed and are environmental friendly and define the soil characteristics that are needed to estimate the soil response.

### 3 SEISMIC NOISE ANALYSIS AND SITE CHARACTERIZATION

Working in an urban environment presents several challenges for seismic measurements due to multiple reasons: presence of various noises (e.g. wind, cars, factories and human movement near the recording stations) and the limitations regarding the type of receiver array geometries that can be used given the limited available space. In such cases, the use of passive seismic noise, as the seismic source is a good option and is, indeed, the main choice in practically all microzonation studies (e.g. Bonnefoy-Claudet, Cotton and Bard 2006; Herak 2009).

There are two main ways to use seismic noise to estimate site effects (e.g. Bonnefoy-Claudet *et al.* 2006;

Chávez-García 2009). The first way is to estimate the local transfer function, which needs 3-component seismic records, with the advantage that the measurement points can be distributed on the study area in a more convenient way. The second way is to estimate the velocity distribution with subsurface depth and, subsequently, to model the site effects. In general, the receivers are installed on an array that can be linear or of any other desired geometry, depending mainly on the analysis technique to be used and the available space. This approach is based on the inversion of the Rayleigh wave dispersion curve derived from measurements, which leads to a one-dimensional subsurface  $V_s$  profile from which parameters such as  $V_{s30}$  and bedrock depth, or sediment thickness, can be determined.

Although these techniques are available and have been used since the late 1950s, better instrumentation and computational resources developed in the last four decades have resulted in a dramatic increase in the quantity and quality of array recording (e.g. Flores Estrella and Aguirre Gonzalez 2003; Scherbaum, Hinzen and Ohrnberger 2003; Bonnefoy-Claudet *et al.* 2006; Kanli *et al.* 2006; Mohamed *et al.* 2013; Hollender *et al.* 2018; Vicêncio, Teves-Costa and Sá Caetano 2018; Mahajan and Kumar 2018; Pergalani *et al.* 2020; Sairam *et al.* 2019).

Usually, it is accepted that seismic noise has two different origins: natural or cultural, and that the signals differ mainly in their frequency content. At frequencies below 1 Hz, the sources are natural, which includes ocean and large-scale meteorological conditions. At intermediate frequencies, 1–5 Hz, the sources are either natural, such as local meteorological conditions, or anthropic. At higher frequencies, the sources are essentially cultural (anthropic) (Bonnefoy-Claudet *et al.* 2006). Our main interest is the near-surface velocity structure and frequencies ranging from 1 to 30 Hz. Therefore, we assume that ambient seismic noise consists of surface waves generated from natural or anthropic sources (Park *et al.* 2007).

#### 3.1 Analysis techniques: MASW and ReMi

One of the best ways to estimate  $V_{s30}$  in an urban environment such as Guadalajara is to use passive seismic analysis methods such as multichannel analysis of surface waves (MASW) (Park *et al.* 1999; Park *et al.* 2007) and refraction microtremors (ReMi) (Louie 2001). These methods allow us to determine shallow subsurface shear-wave velocity profiles in a non-invasive and environmental-friendly way.

The MASW was originally proposed as an active seismic method that uses an active seismic source, a linear receiver

array and a roll-along mode of data collection (Park *et al.* 1999). However, the need to increase the investigation depth and have simpler receiver arrays, especially in urban areas, led to the adaptation of the method for use with passive seismic sources; specifically, ambient seismic noise (Park *et al.* 2007). This new methodology is similar to that used for ReMi. Both methods currently use traditional seismic reflection/refraction equipment (Stephenson *et al.* 2006) with 12 or more vertical geophones forming a linear array. The measurement-analysis procedures are also similar: specifically, (i) multichannel acquisition of seismic noise; (ii) extraction of dispersion curves of Rayleigh waves; and (iii) inversion of these dispersion curves to obtain  $V_S$  profiles (Park *et al.* 2007). Furthermore, Stephenson *et al.* (2005) concluded that the results of ReMi and MASW are comparable for depths less than  $\sim 30$  m.

For this study, we analyse seismic noise data from two measurement campaigns during which we use a linear array of 24 vertical geophones with a geophone spacing of 3–5 m. The first campaign consists of 23 measurement sites, ReMi sites 11–33 in Table 1, and covers an area of approximately 90 km<sup>2</sup>, which is less than 20% of the urban area of Guadalajara. The second campaign consists of 10 measurement sites, MASW sites in 1–10 in Table 1. The simultaneous use of these two campaigns allows us to analyse the seismic response for a large part of the urban area of Guadalajara.

### 3.2 $V_{S30}$ classification

Borcherdt (1992, 1994) uses the parameter  $V_{S30}$  to provide a definition of site classes and site coefficients for the estimation of site-dependent response spectra in accordance with National Earthquake Hazards Reduction Program (NEHRP) (BSSC 2009). Presently,  $V_{S30}$  is a well-accepted and robust parameter used to characterize local site response (e.g. Kanli *et al.* 2006; Rošer and Gosar 2010; Hollender *et al.* 2018; Sairam *et al.* 2019). It is used for building codes, earthquake resistant design, shake maps or, like in this work, to define a seismic zonation within an urban area.

$V_{S30}$  is obtained using the following equation:

$$V_s = \frac{\sum_{i=1}^n d_i}{\sum_{i=1}^n \frac{d_i}{V_{si}}}, \quad (1)$$

where  $d_i$  denotes the thickness of the  $i$ th layer whose depth lies between 0 and 30 m, and  $V_{si}$  denotes the shear wave velocity of the  $i$ th layer in m/s. In Table 2, we show the soil classifications in accordance with the NEHRP (BSSC 2009). For this study, we obtain values of  $V_{S30}$  from near-surface velocity profiles estimated from the seismic noise analysis us-

ing the refraction microtremors and multichannel analysis of surface waves methodologies.

### 3.3 Fundamental soil period estimation

When earthquake waves propagate through soils, the ground motion amplification depends mainly on the fundamental period of the soil,  $T_S$ . Therefore,  $T_S$  is an essential parameter to estimate possible site effects during future earthquakes. There are different techniques to estimate  $T_S$ , most of them employ an analysis of seismic event records to obtain spectral ratios between the vertical and the horizontal components (Lermo and Chávez-García 1993). However, this is only possible if there exists a seismological network with several event records.

In case there are no seismic records available, it is possible to estimate  $T_S$  by assuming a uniform layer of soil overlying rigid bedrock. Considering a constant shear wave velocity down to a depth  $H$ , the natural period,  $T_{sn}$ , for the  $n$ th mode of vibration is given by (Kramer 1996; Yoshida 2015):

$$T_{sn} = \frac{4H}{V_s(2n-1)}, \quad (2)$$

where  $H$  denotes the soil thickness and  $V_s$  denotes the average shear wave velocity of the soil.

The fundamental soil period,  $T_s$ , is defined as the natural period corresponding to the fundamental mode,  $n = 1$ . Substituting  $n = 1$  into equation (2) yields the equation for  $T_s$ , namely:

$$T_s = \frac{4H}{V_s}. \quad (3)$$

According to the NEHRP classification (BSSC 2009) shown in Table 2, a site with a  $V_s \geq 760$  m/s is considered to be rock. Therefore, we can assume that  $H$  in equation (2) corresponds to the depth where  $V_s \geq 760$  m/s. We extract this information from the inverted velocity profiles obtained from multichannel analysis of surface waves and refraction microtremors (see Table 1).

We use the three parameters,  $V_{S30}$ ,  $T_s$ , and bedrock depth, estimated in this work for each of the 33 sites to create the respective interpolated maps. From a variety of interpolation methods, we choose the kriging method (Krige 1951; Matheron 1963, 1973; Angung and Tamia 2013) to interpolate between the data points because it is commonly used in geostatistical and engineering analysis (e.g. Philip and Watson 1982; Watson and Philip 1985; Angung and Tamia 2013).

On all of the resulting maps shown in the various figures, we superimpose the urban area of Guadalajara

**Table 1** List of 33 sites under study in Guadalajara, stations name and main results from the seismic noise analysis

No	Location Name	Station	$V_{S30}$ (m/s)	NEHRP	Bedrock Depth (m)	$T_S$ (s)
1	Arcos Vallarta	ARCO	282	D	52	0.6
2	Colegio de Ingenieros	CICEJ	279	D	40	0.41
3	Ciudad granjas	GRAN	265	D	52	1.04
4	Jardines del sur	JARDS	203	D	115	0.66
5	Oblatos	OBLA	428	C	15	0.14
6	Obras Publicas Zapopan	OPZA	290	D	105.7	0.46
7	Planetario	PLAN	453	C	17	0.15
8	Rotonda	ROTO	268	D	35	0.49
9	San Rafael	SRAF	477	C	12.5	0.1
10	Tonala	TONA	900	B	1	0.1
11	Colegio Cervantes	GDLC	400	C	40	0.39
12	UP campus Guadalajara	GDLP	321	D	62	0.77
13	Catedral	CATR	262	D	31	0.47
14	Antigua Biblioteca Pública	ABIB	260	D	25	0.38
15	Registro Civil No. 1	REGC	318	D	32	0.4
16	Fco. Javier y Lerdo de Tejada	LERD	311	D	50	0.64
17	Hotel Riu Plaza Guadalajara	HRIU	324	D	54	0.67
18	La Gran Plaza	GPZA	357	D	60	0.67
19	Patria y Guadalupe	PATG	339	D	45	0.53
20	Lopez Mateos y Mariano Otero	LMAT	339	D	84	0.99
21	Colomos y Manuel M. Dieguez	COLO	329	D	31	0.38
22	Eulogio Parra y Pablo Casals	PARR	353	D	60	0.68
23	Pablo Neruda y Paseo Jacarandas	NERU	319	D	33	0.41
24	Punto Sao Paulo	SAOP	557	C	9	0.06
25	Patria y Eva Briseño	EVAB	425	C	17	0.16
26	Patria y Paseo Royal Country	ROYA	395	C	46	0.47
27	Paseo V. Real y Servidor Público	REAL	424	C	38	0.36
28	Perifetico y Laureles	LAUR	396	C	72	0.73
29	Nueva Biblioteca Pública	NBIB	301	D	37	0.49
30	Federalismo y Fransisco Villa	VILLA	303	D	27	0.38
31	Lazaro Cardenas y Ferrocarril	FERRO	463	C	9	0.1
32	Real Tulipanes	TULIP	311	D	27	0.42
33	Solares	SOLAR	318	D	85	1.19

(neighbourhoods, blocks and streets). By doing so,  $V_{S30}$ ,  $T_S$  and bedrock depth can be determined more easily for each of the 90 neighbourhoods, 900 blocks and 400 streets of the city, thus making the maps more useful for local authorities, structural designers and constructors.

#### 4 DATA AND RESULTS

The 33 sites in Guadalajara where we measure seismic noise are shown in Figure 2. At each site, we record using linear arrays of 12–24 vertical geophones, a sample rate of 200 samples per second and a receiver spacing of 1–5 m, depending on the conditions at each site. In Figure 3, we show an example of the data recorded at station Rotonda (station number 8, see Fig. 2) for 10 channels and a recording time of 1 min.

At sites 1 through 10 (see Fig. 2), we apply the multichannel analysis of surface waves analysis, and at sites 11 through 33 (see Fig. 2), we apply the refraction microtremors analysis. The blue numbers in Figure 2 indicate the 18 sites located in the western part of the city where tall buildings predominate. For each point, we first obtain the  $V_s$  profile to estimate  $V_{S30}$  (equation (2)) and  $T_S$  (equation (3)). Next, we construct the NEHRP classification and isoperiod maps shown in Figures 4 and 5, respectively.

According to the  $V_{S30}$  values and the resultant soil classification (Fig. 4 and Table 1), we have soil type B at one site, C at 12 sites and D at 20 sites. From the isoperiod map (Fig. 5), we have  $T_S$  values lying between 0.1 s and 1.19 s. We observe that  $T_S$  increases gradually from east to west, and that three dominant regions are defined: the first is a vast area located in

**Table 2** NEHRP Soil profile type classifications as a function of the average shear wave velocity to 30 m depth,  $V_{S30}$  (BSSC 2009)

Soil Type	General Description	$V_{S30}$ (m/s)
A	Hard rock	$V_{S30} > 1500$
B	Rock	$760 < V_{S30} < 1500$
C	Very dense soil and soft rock	$360 < V_{S30} < 760$
D	Stiff soil $15 < N < 50$ or $50 > 100$ kPa ( $N =$ SPT blow count)	$180 < V_{S30} < 360$
E	Soil or any profile with more than 3 m of soft clay defined as soil with $PI > 20$ , $w > 40\%$ and $S_u < \text{kPa}$	$V_{S30} < 180$
F	Soils requiring site-specific evaluations	

Abbreviations: PI, plasticity index;  $S_u$ , undrained shear strength;  $w$ , water content.

the eastern part of Guadalajara within which  $T_S$  values range from 0.05 s to 0.2 s (grey area), followed by a second region within which  $T_S$  values range from 0.2 s to 0.6 s (green area), which is in turn followed by a third region within which  $T_S$  values range from 0.6 s to 1.2 s (yellow and orange areas).

With the bedrock depth information in Table 1 and a digital elevation model, we generate a three-dimensional surface map of Guadalajara, stacking surface and bedrock depth layers (Fig. 6). The upper panel in Figure 6 presents the estimated bedrock depth. The lower panel shows an elevation map of the city which illustrates that Guadalajara is flanked to the east and west by two high elevations, marked as orange areas, which enclose a depression denoted by green and grey areas located just in the centre of the city. Figures 7 and 8 show N–S and E–W profiles across the city, respectively. The comparison between profiles A–A\* and B–B\* (Fig. 7) shows that the soil thickness increases towards the west part of the

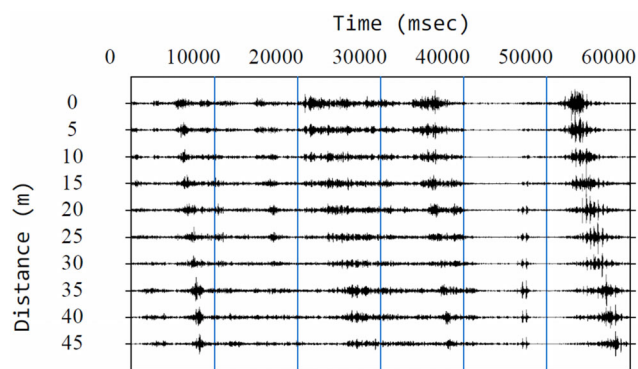


**Figure 3** Example of the data recorded at Station Rotonda (station number 8) for 10 channels and a recording time of 1 min.

city. Similarly, profiles C–C\* and D–D\* (Fig. 8) show thicker soils to the west and to the south.

#### 4.1 Special cases

During the seismic noise analysis, we encountered several special cases that warrant further discussion and analysis. The first such case, discussed in Section 4.1.1, refers to stations Rotonda and Catedral (see Fig. 2 and Table 1). These stations give us the opportunity to compare the results of the multi-channel analysis of surface waves and refraction microtremors methods. The second such case, discussed in Section 4.1.2, refers to stations Oblatos, Planetario and Tonalá, stations 5, 7 and 10, respectively. These stations lack dispersive features.

##### 4.1.1 Stations Rotonda and Catedral

The stations Rotonda and Catedral are quite close to each other,  $\sim 15$  m apart (Fig. 2). However, we analysed the data from Rotonda (station 8) and Catedral (station 13) using the multichannel analysis of surface waves and refraction (MASW) and refraction microtremors (ReMi) methodologies, respectively. This gives us the opportunity to compare the results of the two analysis methods (Table 4). The  $V_{S30}$  estimation for the two stations is nearly identical: the MASW site, Rotonda, has a  $V_{S30} = 268$  m/s and the ReMi site, Catedral, has a  $V_{S30} = 262$  m/s. This supports our assumption that the two methods yield similar results, and we can clearly classify both sites as soil type D of the NEHRP (BSSC 2009). The estimated bedrock depth determined with MASW at Rotonda is 35 m and that determined with ReMi at Catedral is 31 m, again very similar. Furthermore, using equation (3) and the results from the velocity profiles, we estimate  $T_S$  to be 0.51 s and 0.47 s for Rotonda and Catedral, respectively. These values again show that the results of the two analysis methods are very consistent.

##### 4.1.2 Stations Tonalá, Oblatos and Planetario

For station Tonalá, station number 10 in Table 1, we obtain no dispersion curve from the multichannel analysis of surface waves and refraction analysis. A previous study (Chavez *et al.* 2014) gives a bedrock depth of  $\sim 0.75$  m for this location. Such a shallow bedrock depth could explain the absence of dispersive features. Therefore, we classify this station as type B (BSSC 2009). For stations Oblatos and Planetario, stations 5 and 7 in Table 1, respectively, although we obtain a dispersion curve, which we invert to estimate  $V_{S30}$ , it is not possible to

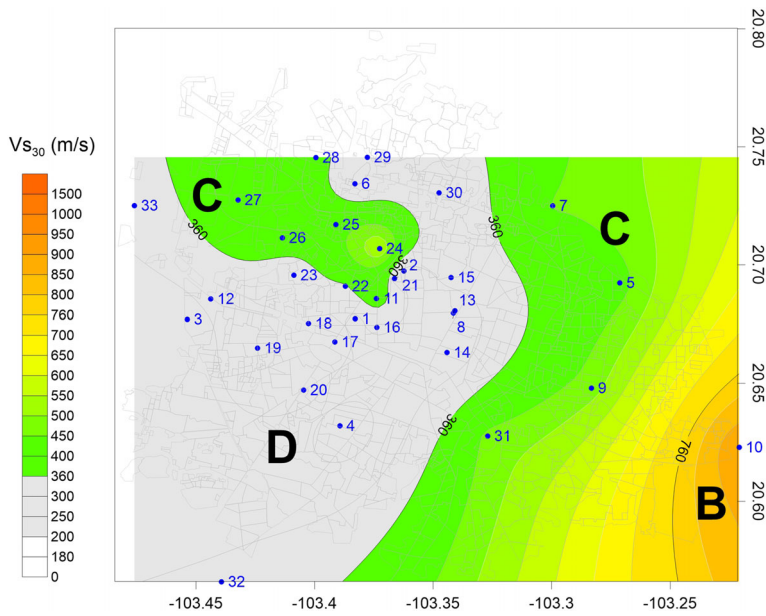


Figure 4  $V_{S30}$  interpolation map for the 33 sites under study in Guadalajara and site classification according with NEHRP (BSSC 2009). Background map is the urban area of Guadalajara (neighbourhoods, blocks and streets).

estimate the bedrock depth. Therefore, we accept the values proposed by Chavez *et al.* (2014), namely 15 m for Oblatos and 17 m for Planetario.

### 5 DISCUSSION

Our near-surface seismic noise analysis on the pumice soils in Guadalajara shows that at one site the soil can be classified as type B, type C at 12 sites and type D at 20 sites.

However, Mesri and Vardhanabhuti (2009) classified pumice soils as type C, with a behaviour similar to carbonate sands. The reason for this discrepancy is not clear; however, a likely explanation for the degradation of type C to type D soils at 20 sites in Guadalajara may be the presences of sand and/or lime within the sediments.

We calculate the fundamental periods using equation (3) and the results of the velocity profiles from the surface wave analysis (Table 1). The isoperiod map can be used to

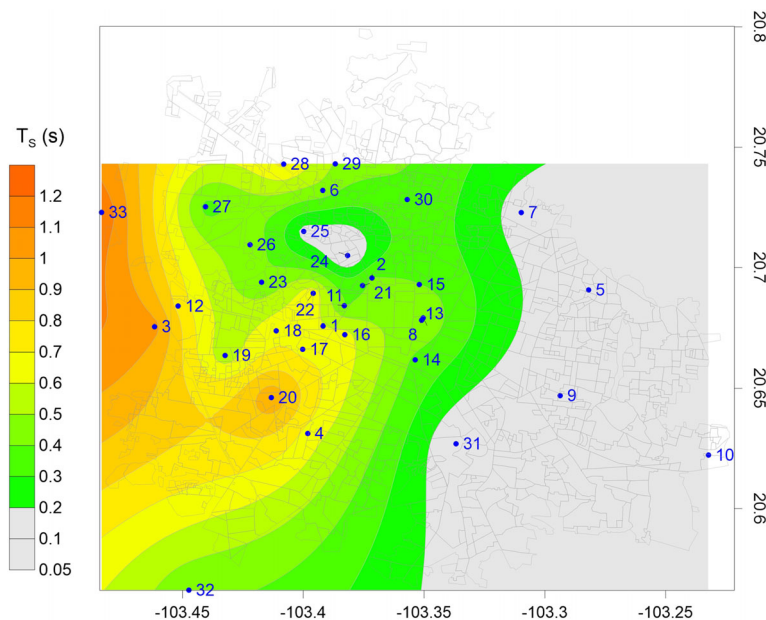
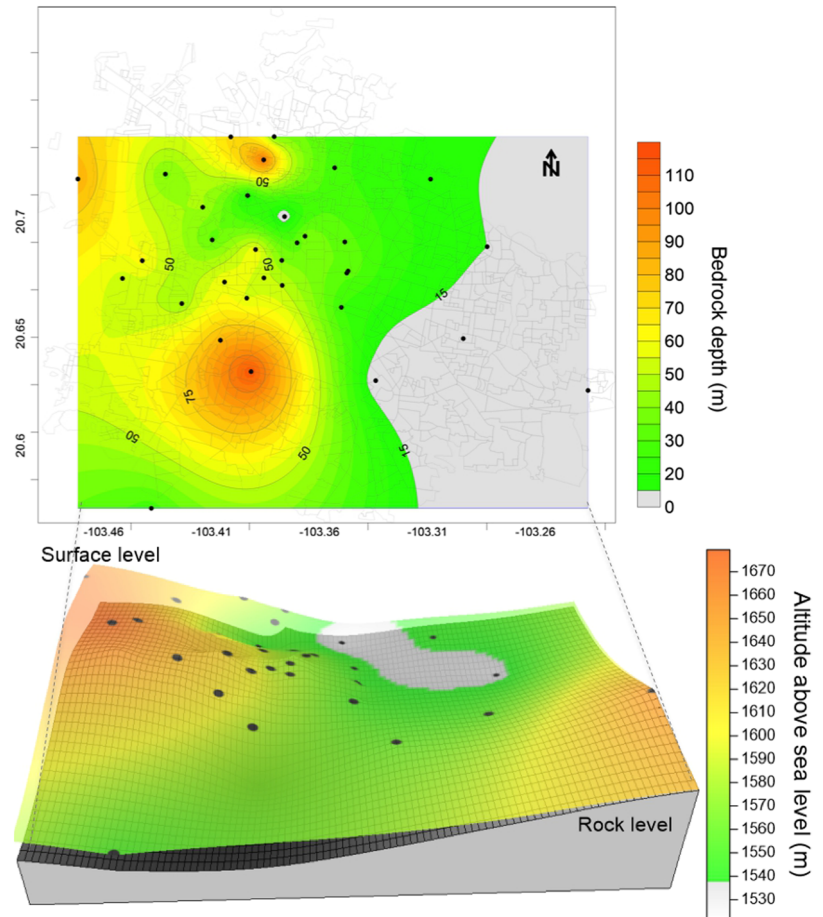


Figure 5  $T_s$  interpolation map for the 33 sites under study in Guadalajara. Background map is the urban area of Guadalajara (neighbourhoods, blocks and streets).

**Figure 6** Three-dimensional surface map of Guadalajara stacking surface and bedrock layers. Scale bar shows the elevation of surface layer related to maximum depression of bedrock layer. Upper inset figure shows the interpolated bedrock depth superimposed on the map of the urban area of Guadalajara (neighbourhoods, blocks and streets).



estimate the resonant vulnerability for different types of structures with different heights. In order to validate the results of our fundamental period analysis, we estimate this parameter from H/V spectral ratios (HVSr) for the S-wave part of seismological records from stations Rotonda (ROTO) and UP campus Guadalajara (GDLP). For ROTO, we use the seismological record of the 1995 Manzanillo earthquake, Mw 8.1. For GDLP, we use the events listed in Table 3.

In Figure 9, we compare the  $T_s$  estimates obtained from HVSr with those calculated using equation (3) and the velocity profiles. In Figure 9(a), the main peak of HVSr for the Manzanillo earthquake at ROTO is well marked at 0.49 s, which is in good agreement with our calculated value of  $T_s$  (see Table 4). The estimates obtained from HVSr for GDLP illustrated in Figure 9(b) shows two peaks at 0.7 and 0.91 s. The first peak is in good agreement with our calculated value of  $T_s$ . The second peak ( $\sim 0.9$  s) is probably due to a more complex structure or changes in the velocity structure that cannot be defined with surface wave analysis methods. The similarity of

the  $T_s$  values at both stations shows the consistency between the results of the surface wave analysis methods (ReMi and MASW) and seismic data, and serves to validate our results.

Based on the estimated bedrock depth (Table 1), which is equivalent to soil thickness, we propose a new geotechnical microzonation for Guadalajara consisting of four zones (see Table 5 and Fig. 10). It is well known that the site response is intrinsically linked to structural design. For this reason, in Figure 10 we superimpose our proposed geotechnical zonation of Guadalajara with the predominant construction types found in the city.

We classify the constructions of Guadalajara in three categories based on age, number of stories and construction type as follows:

- Category 1: 1–4 storied buildings, constructed of masonry and concrete, and older than 50 years. These are represented with black triangles in Figure 10. They are located predominantly in geotechnical zone I, with a few located at the northern part of geotechnical zone II.



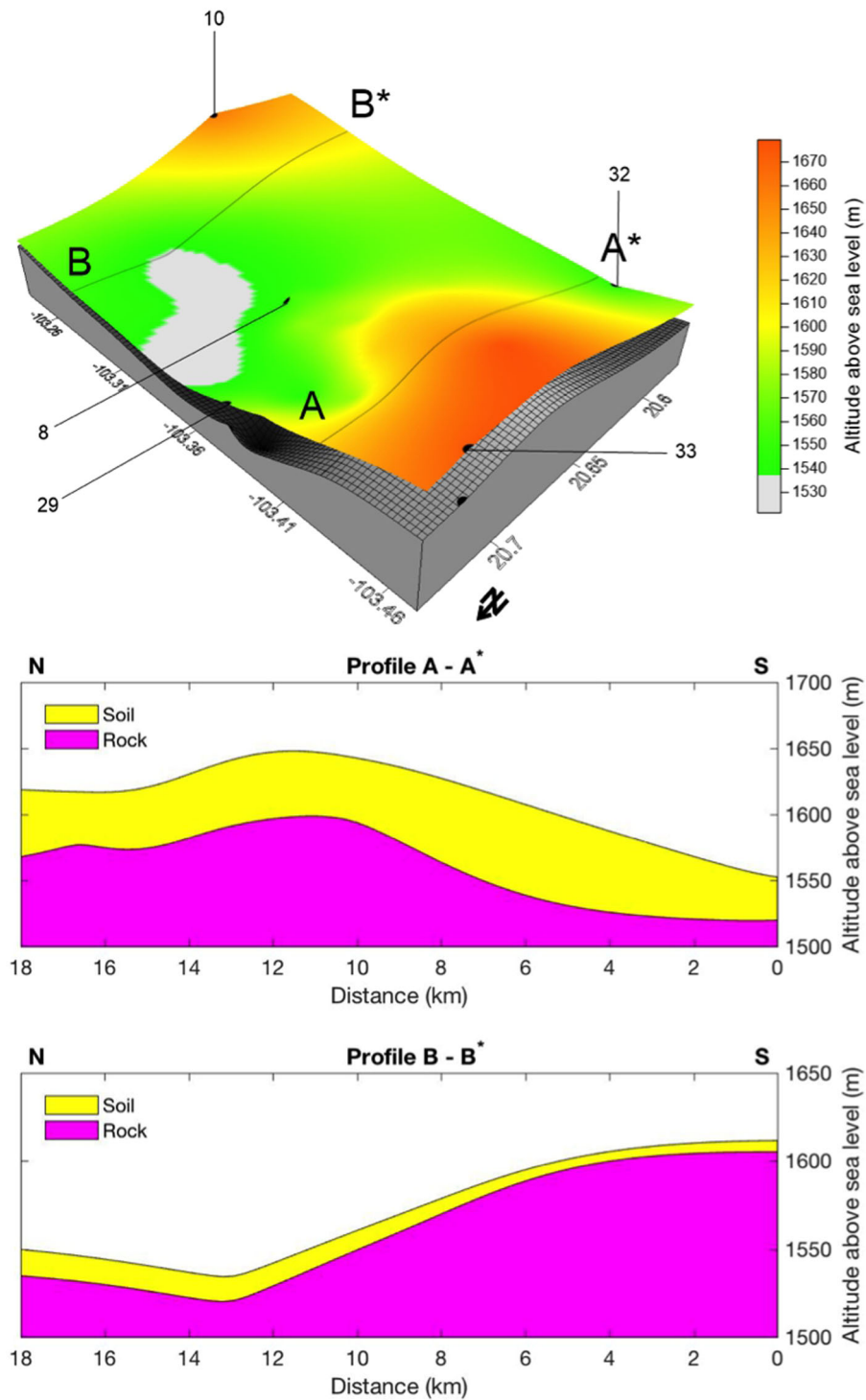


**Figure 7** Soil profiles in direction North–South for Guadalajara. (Top) Three-dimensional surface map of the city stacking surface and bedrock layers. Thin continuous lines indicate the orientation of profiles plotted in (centre) and (bottom). (Centre) Soil profile along line A-A\*. (Bottom) Soil profile along line B-B\*. The location of the five stations referred to in the text is displayed (one in each border and one in the centre of the city).

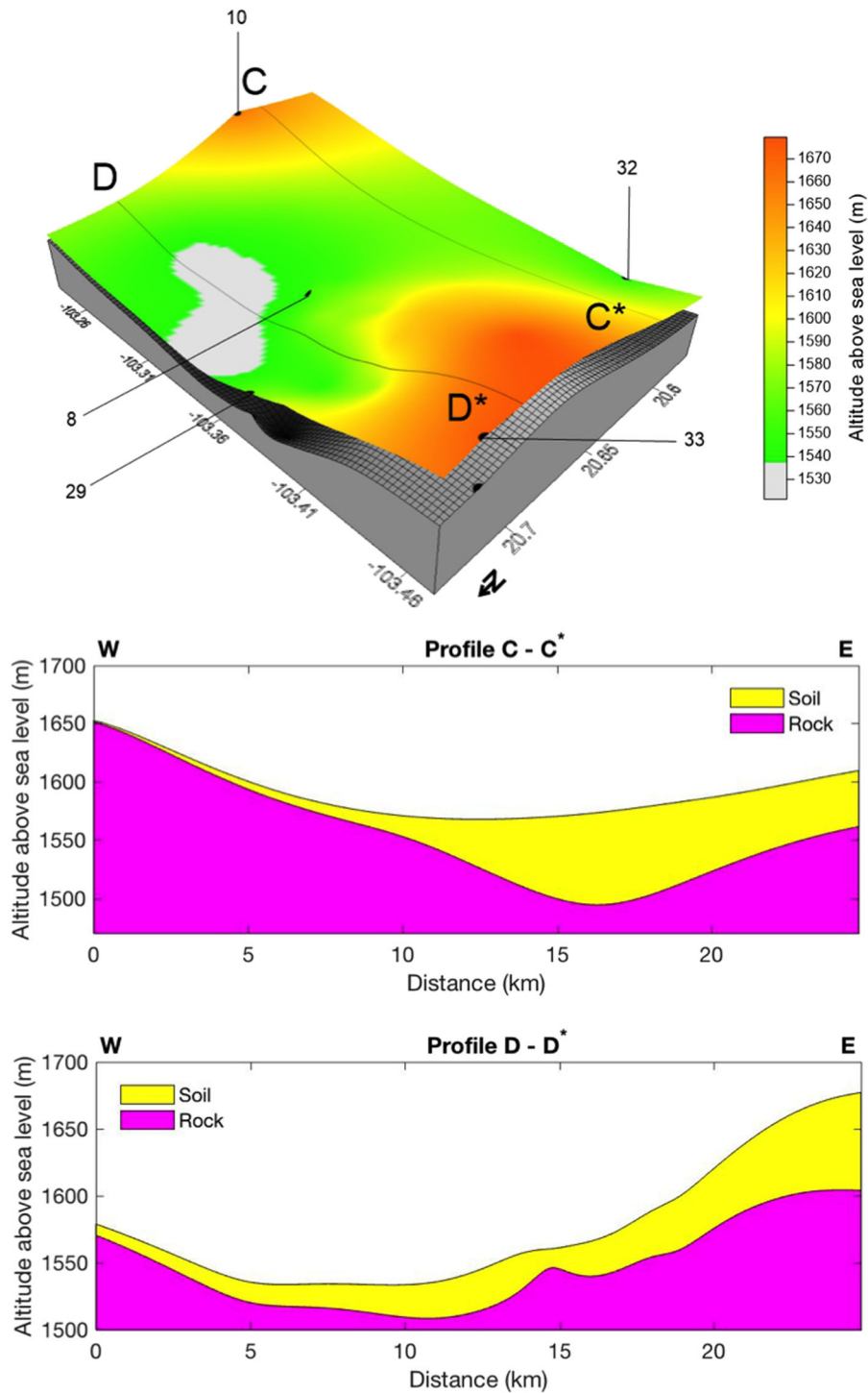


**Figure 8** Soil profiles in direction East–West for Guadalajara. (Top) Three-dimensional surface map of the city stacking surface and bedrock layers. Thin continuous lines indicate the orientation of profiles plotted in (centre) and (bottom). (Centre) Soil profile along line C-C\*. (Bottom) Soil profile along line D-D\*. The location of the five stations referred to in the text is displayed (one in each border and one in the centre of the city).

**Table 3** Date, time and magnitude of the events recorded in station GDLP to estimate the fundamental period by H/V spectral ratios

No.	Date (dd-mm-yyyy)	Time (hh:mm:ss)	Magnitude (Mw)
1	22-04-2013	01:16:34	5.8
2	15-12-2015	16:09:23	4.4
3	15-12-2015	16:32:35	3.6
4	15-12-2015	17:49:48	3.9
5	17-12-2015	07:59:12	4.1
6	11-05-2016	22:35:18	4.8

- Category 2: 1–50 storied buildings, constructed of reinforced concrete, steel or concrete frames, which were built in the last 30 years. Those with more than 40 stories were built within the last 10 years. These appear as black diamonds in Figure 10 and are distributed in geotechnical zones II, III and IV.
- Category 3: Very old buildings (80–300 years), mainly constructed of mud, adobe or quarry, without concrete or steel. These are mainly churches, old hospitals, monuments and large houses constructed during the colonial period (XV–XVII centuries). These are shown as black asterisks in Figure 10 and are mainly located in geotechnical zone II.

The structures of Category 1 have a structural period,  $T_E$ , between 0.1 and 0.4 s (Preciado *et al.* 2017; Ramirez-Gaytan *et al.* 2019). They are located mainly within the geotechnical zone with  $0.05 > T_S > 0.3$  s (see Fig. 5), and within the shallowest bedrock depth ( $\leq 15$  m) region. Therefore, most of the constructions in this area have a  $T_E$  similar to  $T_S$ . Consequently, the occurrence of the resonance phenomena is possible during a future intermediate to strong earthquake. Although this area has no big economic growth, it is the area with the highest population density in the city.

Category 2 constructions have a  $T_E$  between 0.1 and 5 s (Preciado *et al.* 2017; Ramirez-Gaytan *et al.* 2019). They are located mostly in geotechnical zones II, III and IV, where  $T_S$  varies from 0.2 to 1.2 s, and in the region with medium to large

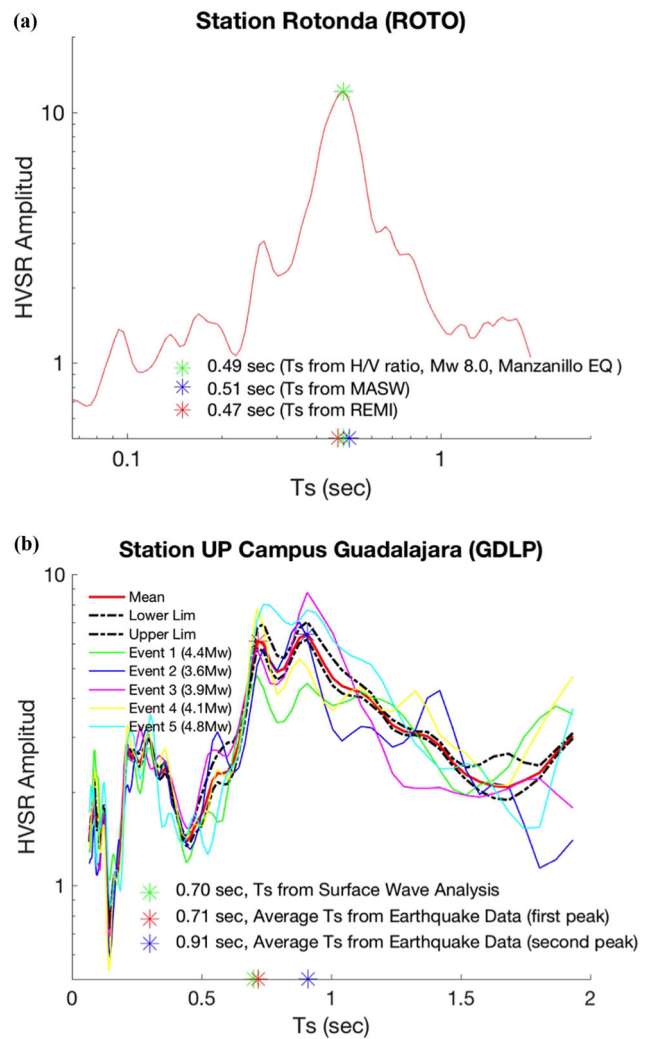


**Figure 9** Comparison of  $T_s$  obtained from surface wave analysis versus  $T_s$  from earthquake data. (a) Comparison of  $T_s$  from MASW and ReMi in station Rotonda versus  $T_s$  from H/V spectral ratios from Manzanillo earthquake MW 8.1. (b) Comparison of average  $T_s$  from H/V spectral ratios of five events versus  $T_s$  from ReMi in GDLP station.

**Table 4** Results of the comparison of  $V_{S30}$ ,  $T_s$  and bedrock depth for stations Rotonda and Catedral (station numbers 8 and 13, respectively). The analysis with different methodologies all produced similar results, which also agree with the results using the H/V spectral ratio for the event of Manzanillo, 1995 (Mw 8.1)

No.	Location	Name	$V_{S30}$	NEHRP	Bedrock Depth (m)		$T_s$ (s)	
					REMI	MASW	$T_s = 4$ H/V	H/V
8	Rotonda	ROTO	268	D	–	35	0.51	0.49
13	Catedral	CATR	262	D	31	–	0.47	–

**Table 5** Zonation in terms of the bedrock depth (i.e. soil thickness)

Zone	Bedrock Depth, brdepth (m)
I	$\text{brdepth} \leq 15$
II	$15 < \text{brdepth} \leq 50$
III	$50 < \text{brdepth} \leq 75$
IV	$\text{brdepth} > 75$

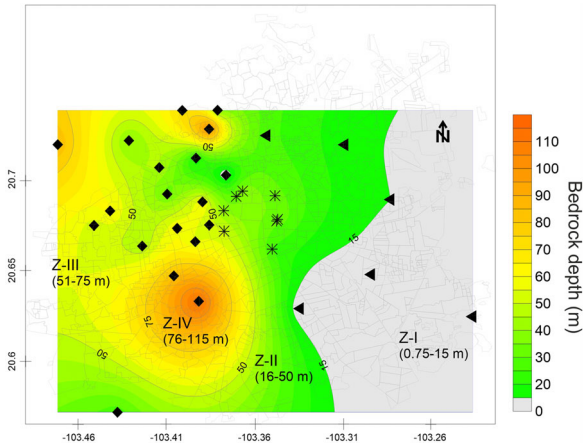


**Figure 10** Geotechnical microzonation of Guadalajara in four zones (colour interpolation) superimposed on the Guadalajara street map. Scale bar shows the bedrock depth. Black triangles, asterisks and diamonds represent the three different construction systems detailed in the text. Background is the urban area of Guadalajara (neighbourhoods, blocks and streets).

bedrock depths (16–115 m). The fact that constructions with 1–12 stories have a  $T_E$  within the range of  $T_S$  increases the possibility that the resonance phenomena will occur during intermediate to strong earthquakes. It is worth noting that the tallest buildings are located in these three geotechnical zones, and that these neighbourhoods have the highest economic growth in the city.

Finally, Category 3 constructions have a  $T_E \approx 0.4$  s (Prezado *et al.* 2017; Ramirez-Gaytan *et al.* 2019), and are located mainly on geotechnical zones with  $0.6 > T_S > 0.2$  s and with medium bedrock depths (15–60 m). We classify these constructions as the most vulnerable to a severe earthquake, not only because their  $T_E$  falls within the range of  $T_S$  which implies possible resonance phenomena, but also because their construction materials are quite brittle, old and without structural integrity.

## 6 CONCLUSIONS

Guadalajara is probably the largest city in the world with a subsurface composed of pumice soils. Their fragile com-

position increases the difficulty to carry out geotechnical characterization applying the traditional mechanical methods. Therefore, the use of passive seismic analysis techniques is arguably the best alternative to characterize this type of soil.

We obtain the soil classification based on  $V_{S30}$  at 33 measurement locations in Guadalajara, which results in the definition of three soil types. Moreover, using the information of the velocity profiles, we define an isoperiod map that delineates three distinct regions in the city: the first region is a vast area to the east with  $0.2 > T_S > 0.05$  s, followed by a second region with  $0.6 > T_S > 0.2$  s, and a third region with  $1.2 > T_S > 0.6$  s.

Based on these results and the estimated bedrock depth obtained from the velocity profiles, we propose a geotechnical zonation for Guadalajara. The four regions are correlated with the different structural designs of the constructions in the city, which are also classified into three categories. This analysis shows the areas of the city where the resonance phenomena are expected to occur during an intermediate to strong earthquake.

We expect that the maps resulting from our work will be of great value to structural engineers and local authorities, who can use these maps as a fundamental tool to prevent major structural damage and human casualties during moderate to strong earthquakes. Structural engineers can use the information about fundamental soil periods at different sites of the city to diminish or avoid the resonance vulnerability for existing and new buildings. It is desirable that new local seismic codes and construction licenses incorporate these results to define the maximum building height and the needed structural systems to avoid the resonance phenomena and, thus, to avoid major structural damage and sudden collapses.


These results also provide a good basis for further studies to evaluate the interaction between soil and structure for Guadalajara, especially for collecting more measurements to construct more detailed maps. We recommend assessing ratios between structural period  $T_E$  and soil period  $T_S$  as an initial check of the structural safety of any edification in the city.

## ACKNOWLEDGEMENTS

We appreciate the support of the Unidad de Instrumentacion Sismica of the Instituto de Ingenieria (IINGEN) of the Universidad Nacional Autonoma de Mexico (UNAM) that provided the acceleration records of the 1995 Manzanillo earthquake (Mw 8.0) in the city of Guadalajara. This research was developed in collaboration with the Cuerpo Academico UDG-CA-941 Ciencias de la Tierra–Peligros Naturales of the

Universidad de Guadalajara. This research was partially supported through the project Evaluación de Vulnerabilidad Sísmica en Puerto Vallarta (PRODEP Fortalecimiento de Cuerpos Académicos, UDG-CA-941, IDCA 28289). We thank the reviewers, editors and production staff for their help in improving the manuscript.


## ORCID


Alejandro Ramírez Gaytan 

<https://orcid.org/0000-0001-7602-2714>


Hortencia Flores Estrella 

<https://orcid.org/0000-0001-8201-7655>

Adolfo Preciado  <https://orcid.org/0000-0002-5430-2034>

William L. Bandy 

<https://orcid.org/0000-0002-2773-4069>

Michael Korn  <https://orcid.org/0000-0003-1230-9016>

## REFERENCES

- Angung S. and Tamia T. 2013. Comparison of kriging and inverse distance weighted (IDW) interpolation methods in lineament extraction and analysis. *Journal of Southeast Asian Applied Geology* 5, 21–29.
- Bonnefoy-Claudet, S., Cotton, F. and Bard P.Y. 2006. The nature of noise wavefield and its applications for site effects studies: a literature review. *Earth-Science Reviews* 79, 205–227.
- Borcherdt R. 1992. Simplified site classes and empirical amplification factors for site-dependent code provisions. NCEER, SEAOC, BSSC workshop on site response during earthquakes and seismic code provisions, University of Southern California, Los Angeles, California, November 1992.
- Borcherdt R. 1994. Estimates of site-dependent response spectra for design (methodology and justification). *Earthquake Spectra* 10, 617–654.
- Brooms B. and Floding N. 1988. History of soil penetration testing. *Proceedings of the 1st International Symposium on Penetration Testing, Orlando, FL*, pp. 157–220.
- BSSC 2009. NEHRP recommended provisions for seismic regulations for new buildings and other structures. Part1: provisions (FEMA 368). Federal Emergency Management Agency, Washington, DC.
- Castillo-Aja R. and Ramírez-Herrera M. 2017. Updated tsunami catalog for the Jalisco-Colima coast, Mexico, using data from historical archives. *Seismological Research Letters* 88, 144–158.
- Chavez M., Garcia S., Cabrera E., Ashworth M., Perea N., Salazar A. et al. 2014. Site effects and peak ground accelerations observed in Guadalajara, Mexico, for the 9 October 1995 Mw 8 Colima-Jalisco Earthquake. *Bulletin of the Seismological Society of America* 104, 646–656.
- Chávez-García F.J. 2009. Ambient noise and site response: from estimation of site effects to determination of the subsoil structure. In: *Increasing Seismic Safety by Combining Engineering Technologies and Seismological Data* (eds M. Mucciarelli, M. Herak and J. Cassidy) pp. 53–71. Springer, Dordrecht.
- Flores Estrella H. and Aguirre Gonzalez J. 2003. SPAC: an alternative method to estimate earthquake site effects in Mexico City. *Geofísica Internacional* 42, 227–236.
- Flores-Estrella H., Lomnitz C. and Yussim S. 2007. Seismic response of Mexico City Basin: a review of twenty years of research. *Natural Hazards* 40, 357–372.
- García A. and Suárez R. 1996. Los sismos en la historia de México. Universidad Nacional Autónoma de México, Centro de Investigaciones y Estudios Superiores en Antropología Social, and Fondo de Cultura Económica, México D. F. 718 (In Spanish).
- Herak M. 2009. The use of ambient noise for building and soil characterisation. In: *Increasing Seismic Safety by Combining Engineering Technologies and Seismological Data* (eds M. Mucciarelli, M. Herak and J. Cassidy) pp. 1–2. Springer, Dordrecht.
- Hollender F., Cornou C., Dechamo A., Oghalaei K., Renalier F., Maufroy E. et al. 2018. Characterization of site conditions (soil class, VS30, velocity profiles) for 33 stations from the French permanent accelerometric network (RAP) using surface wave methods. *Bulletin of Earthquake Engineering* 16, 2337–2365.
- Kanli A.I., Tildy P., Prónay Z., Pinar A. and Hermann L. 2006. Vs<sup>30</sup> mapping and soil classification for seismic site effect evaluation in Dinar region, SW Turkey. *Geophysical Journal International* 165, 223–235.
- Kramer S. 1996. *Geotechnical Earthquake Engineering*. Pearson, London.
- Krige D. 1951. *A statistical approach to some mine valuations and allied problems at the Witwatersrand*. Master's thesis, University of Witwatersrand, South Africa.
- Lazcano S. 1995. Experiencias con cono dinámico en suelos pumíticos. Memorias del X congreso panamericano de mecánica de suelos e ingeniería de cimentaciones, *Guadalajara Mexico* 1, 244–251. (In Spanish.)
- Lazcano S. 2001. Sismicidad histórica de Guadalajara. XIII Conferencia nacional de ingeniería Sísmica. Guadalajara, México. (In Spanish.)
- Lazcano S. 2004. Contexto histórico y geotécnico de Guadalajara. Memorias de la XXII reunión nacional mecánica de suelos. Guadalajara, México 1, 53–66. (In Spanish.)
- Lazcano S. 2007. Caracterización de suelos arenosos mediante análisis de ondas de superficie. Academia Mexicana de Ingeniería. (In Spanish.)
- Lazcano S. 2010. Experiences in pumice soils characterization by surface wave analysis. *Fifth International Conference on Recent Advances in Geotechnical Earthquake Engineering and Soil Dynamics*, San Diego, California, pp. 1–9.
- Lermo J. and Chávez-García F. 1993. Site effect evaluation using spectral ratios with only one station. *Bulletin of the Seismological Society of America* 83, 1574–1594.
- Louie J. 2001. Faster, better: shear-wave velocity to 100 meters depth from refraction microtremors arrays. *Bulletin of the Seismological Society of America* 91, 347–364.
- Mahajan A.K. and Kumar P. 2018. Site characterisation in Kangra Valley (NW Himalaya, India) by inversion of H/V spectral ratio

- from ambient noise measurements and its validation by multichannel analysis of surface waves technique. *Near Surface Geophysics* **16**, 314–327.
- Matheron G. 1963. Principles of geostatistics. *Economic Geology* **58**, 1246–1266.
- Matheron G. 1973. The intrinsic random functions and their applications. *Advances in Applied Probability* **5**, 439–468.
- Mesri G. and Vardhanabhuti B. 2009. Compression of granular material. *Canadian Geotechnical Journal* **46**, 369–392.
- Mohamed A.M.E., Abu El Ata A.S.A., Abdel Azim F. and Taha, M.A. 2013. Site-specific shear wave velocity investigation for geotechnical engineering applications using seismic refraction and 2D multichannel analysis of surface waves. *NRIAG Journal of Astronomy and Geophysics* **2**, 88–101.
- Park C., Miller R. and Xia J. 1999. Multi-channel analysis of surface waves. *Geophysics* **64**, 800–808.
- Park C., Miller R., Xia J. and Ivanov J. 2007. Multichannel analysis of surface waves (MASW) active and passive methods. *The Leading Edge* **26**, 60–64.
- Pender M. 2006. Stress relaxation and particle crushing effects during compression of pumice sand. In: *Geomechanics and Geotechnics of Particulate Media* (eds M. Hyodo, H. Murata and Y. Nakata), pp. 91–96. Taylor & Francis, London.
- Pender M., Wesley L., Larkin T. and Pranjoto S. 2006. Geotechnical properties of pumice sand. *Soils and Foundations* **46**, 69–81.
- Pergalani F., Pagliaroli A., Bourdeau C., Compagnoni M., Lenti L., Lualdi M. et al. 2020. Seismic microzoning map: approaches, results and applications after the 2016–2017 Central Italy seismic sequence. *Bulletin of Earthquake Engineering* **18**, 1–35.
- Philip G. and Watson D. 1982. A precise method for determining contoured surfaces. *Australian Petroleum Exploration Association Journal* **22**, 205–212.
- Preciado A. 2011. Seismic vulnerability reduction of historical masonry towers by external prestressing devices. PhD Thesis, Technical University of Braunschweig, Germany and University of Florence, Italy.
- Preciado A., Ramírez-Gaytan A., Lazcano S., Preciado I., Gutiérrez N.Y. and Santos J. 2017. Vulnerabilidad de edificios ante resonancia sísmica en Guadalajara y Zapopan por el sismo del 11 de mayo de 2016 Mw = 4.9. Memorias del XXI Congreso Nacional de Ingeniería Sísmica (SMIS), Septiembre 20–23, Guadalajara, México.
- Quitánar L., Rodríguez Lozoya H.E., Ortega R., Gómez-González M., Domínguez T., Javier C. et al. 2010. Source characteristics of the 22 January 2003  $M_w$  7.5 Tecoman, Mexico, earthquake: new insights. *Pure and Applied Geophysics* **18**, 1339–1353.
- Ramírez-Gaytan A., Aguirre J. and Huerta C. 2010. Simulation of accelerograms, peak ground accelerations, and mmi for the Tecoman earthquake of 21 January 2003. *Bulletin of the Seismological Society of America* **100**, 2163–2173.
- Ramírez-Gaytan A., Preciado A., Bandy W., Salazar-Monroy E., Jaimes M. and Alcántara L. 2019. The Tesisatan, Mexico earthquake (Mw 4.9) of 11 May 2016: seismic tectonic environment and resonance vulnerability on buildings. *Earthquake Engineering and Engineering Vibration* **18**, 579–595.
- Rošer J. and Gosar A. 2010. Determination of Vs30 for seismic ground classification in the Ljubljana area. *Acta Geotechnica Slovenica* **1**, 61–76.
- Sairam B., Singh A.P., Patel V., Chopra S. and Ravi Kumar M. 2019. Vs30 mapping and site characterization in the seismically active intraplate region of Western India: implications for risk mitigation. *Near Surface Geophysics* **17**, 533–546.
- Scherbaum F., Hinzen K.G. and Ohrnberger M. 2003. Determination of shallow shear wave velocity profiles in the Cologne/Germany area using ambient vibrations. *Geophysical Journal International* **152**, 597–612.
- Stephenson W., Louie J., Pullammanappallil S., Williams R. and Odum J. 2005. Blind shear-wave velocity comparison of ReMi and MASW results with boreholes to 200 m in Santa Clara Valley: implications for earthquake ground-motion assessment. *Bulletin of the Seismological Society of America* **95**, 2506–2516.
- Stephenson J., Williams R., Odum J. and Worley D. 2006. Comparison of ReMi, and MASW Shear-wave velocity techniques with a CCOC borehole to 100 m, Santa Clara Valley. United States Geological Survey Open-File Report.
- Suter M. 2015. The A.D. 1567 Mw 7.2 Ameca, Jalisco, earthquake (western trans-Mexican Volcanic Belt): surface rupture parameters, seismogeological effects, and macroseismic intensities from historical sources. *Bulletin of the Seismological Society of America* **105**, 646–656.
- Suter M. 2017. The 2 October 1847  $M_l$  5.7 Chapala graben triggered earthquake (Trans-Mexican Volcanic Belt, west-central Mexico): macroseismic observations and hazard implications. *Seismological Research Letters* **89**, 35–46.
- Vicêncio H., Teves-Costa P. and Sá Caetano P. 2018. Site characterization in Barreiro urban area (Portugal) using H/V and ReMi techniques. *Near Surface Geophysics* **16**, 298–312.
- Watson D. and Philip G. 1985. A refinement of inverse distance weighted interpolation. *Geoprocessing* **2**, 315–327.
- Wesley L., Meyer V., Pranjoto S., Pender M., Larkin T. and Duske C. 1999. Engineering properties of a pumice sand. Proceedings of the 8th Australian New Zealand Conference on Geomechanics: *Consolidating Knowledge*, pp. 901–907. Australian Geomechanics Society.
- Yoshida N. 2015. Seismic Ground response analysis. *Geotechnical, Geological and Earthquake Engineering* **7**, 255–267.
- Zobin V. and Ventura F. 1998. The macroseismic field generated by the Mw 8.0 Jalisco, Mexico earthquake of 9 October 1995. *Bulletin of the Seismological Society of America* **88**, 703–711.